1 2	Deepening of the winter mixed layer in the Canada Basin, Arctic Ocean over 2006- 2017
3	
4	Sylvia T. Cole1, and James Stadler2
5	1Woods Hole Oceanographic Institution, Woods Hole MA.
6	2Haverford College, Haverford PA.
7	
8	
9	
10	
11	
12	
13	
14	
15	
16	
17	
18	
19	
20	
21	
22	
23	
24	Corresponding author: Sylvia Cole (scole@whoi.edu)
25	Key Points:
26 27	• The winter mixed layer in the Canada Basin was 9 m deeper on average over 2013-2017 compared with 2006-2012
28 29	 Mixed layer density increased by 0.5 kg m-3 and stratification at the mixed layer base decreased
30 31 32	 Mixed layer deepening was inferred to result from changes in freshwater accumulation and/or storage that increased mixed layer salinity

Abstract

33

48

60

- 34 The Arctic Ocean mixed layer interacts with the ice cover above and warmer, nutrient rich
- 35 waters below. Ice-Tethered Profiler observations in the Canada Basin of the Arctic Ocean over
- 2006-2017 are used to investigate changes in mixed layer properties. In contrast to decades of 36
- 37 shoaling since at least the 1980's, the mixed layer deepened by 9 m from 2006-2012 to 2013-
- 38 2017. Deepening resulted from an increase in mixed layer salinity that also weakened
- 39 stratification at the base of the mixed layer. Vertical mixing alone can explain less than half of
- 40 the observed change in mixed layer salinity, and so the observed increase in salinity is inferred to
- result from changes in freshwater accumulation via changes to ice-ocean circulation or ice 41
- 42 melt/growth and river runoff. Even though salinity increased, the shallowest density surfaces
- 43 deepened by 5 m on average suggesting that Ekman pumping over this time period remained
- 44 downwards. A deeper mixed layer with weaker stratification has implications for the
- 45 accessibility of heat and nutrients stored in the upper halocline. The extent to which the mixed
- 46 layer will continue to deepen appears to depend primarily on the complex set of processes
- 47 influencing freshwater accumulation.

Plain language summary

- 49 The upper tens of meters of the Arctic Ocean, termed the mixed layer, separate the floating sea
- ice above from warmer and nutrient-rich waters below. Observations in winter are used to 50
- 51 investigate changes to the mixed layer over 2006-2017. The mixed layer has recently gotten
- thicker (deeper) by 9 m, in contrast to past decades where it thinned (shoaled). Deepening 52
- 53 resulted from changes to ocean salinity in the mixed layer that cannot be explained by mixing
- 54 with saltier water below. Thus, the increase in mixed layer salinity is inferred to result from
- interannual changes to the ice-ocean circulation, ice melt/growth, or river runoff. Changes to 55
- 56 water properties also occurred in the region immediately beneath the mixed layer, making it
- 57 energetically easier for heat to be combined into the mixed layer. The extent to which the mixed
- 58 layer will continue to deepen appears to depend primarily on the complex set of processes that
- 59 can influence mixed layer salinity.

1 Introduction

- 61 The Arctic Ocean mixed layer is coupled dynamically and thermodynamically with the ice cover
- 62 above (e.g., McPhee, 2012), while the strong stratification at the mixed layer base effectively
- isolates heat and nutrients from the upper tens of meters of the water column (Maykut and 63
- McPhee, 1995; Shaw et al., 2009). The mixed layer in the Canada Basin is shallow, less than 50 64
- 65 m deep in winter and shoaling to 20 m or less in summer (Toole et al., 2010; Peralta-Ferriz and
- 66 Woodgate, 2015). The shallow winter mixed layer results from limited vertical mixing together
- with buoyant freshwater input (as salinity has the largest influence on density at cold Arctic 67
- 68 temperatures). Freshwater accumulates in the Canada Basin due to the Beaufort Gyre, an
- anticyclonic circulation of the ice and upper ocean driven by surface winds that retains fresh 69
- 70 surface waters via Ekman convergences. Interannual changes to the mixed layer are influenced
- 71 by processes that affect vertical mixing or surface freshwater including: ice melt/growth, river
- 72 runoff, surface circulation, areas of open water (changes to ice extent or leads) where the wind
- 73 can directly force the ocean (Proshutinsky et al. 2009; McPhee et al. 2013; Krishfield et al. 2014;
- 74 Zhang et al. 2016), and internal wave breaking near the mixed layer base (e.g., D'Asaro and
- 75 Morison, 1992). Mixed layer feedbacks with the ice cover make future changes to the Arctic ice

- cover and upper ocean stratification difficult to predict. There is a wide range of potential
- outcomes for the ice cover itself (Carmack et al., 2015), and the nutrients and ecosystems
- 78 residing within and beneath the mixed layer, which are all sensitive to changes in mixed layer
- 79 depth and/or entrainment.
- 80 Observations over 1980-2008 have indicated that the Canada Basin winter mixed layer has
- 81 shoaled due to increased freshwater accumulation. Based on Nov-May observations that are
- 82 interannually sparse, the winter mixed layer trend reported for the period 1980-2008 is a shoaling
- of 0.64 m per year, amounting to 19 m over 30 years (Peralta-Ferriz and Woodgate, 2015).
- Similarly, the trend in winter mixed layer salinity was a freshening of 0.19 psu per year, or 5.5
- psu over 1980-2008 (Peralta-Ferriz and Woodgate, 2015). Freshening extends throughout the
- 86 upper few hundred meters of the water column and has occurred due to increased ice melt and
- 87 river runoff as well as Ekman convergence of surface waters that resulted from increased
- anticyclonic wind stress (Proshutinsky et al., 2009; Krishfield et al., 2014; Zhang et al., 2016).
- 89 Mixed layer shoaling due to freshwater accumulation (and weak vertical mixing) occurred
- simultaneously with increased Ekman pumping that has deepened the average depth of density
- 91 surfaces in the upper halocline (Timmermans et al., 2014; Zhang et al., 2016). Interannual
- 92 changes to freshwater content (and inferred changes to freshwater accumulation) are better
- observed than changes to vertical mixing within or at the base of the mixed layer. It is
- 94 inconclusive to what extent vertical mixing at any depth may be changing interannually (e.g.,
- 95 Guthrie et al., 2013). Whether or at what rate the future mixed layer will continue to shoal is an
- 96 open question.
- 97 Several recent studies have focused on changes to the ice cover and ocean circulation over the
- 98 last decade, but do not address in detail how the mixed layer has been affected. Sea ice extent
- and thickness have continued to decline, with a historic minimum in extent in summer 2012
- 100 (Kwok et al., 2009; Comiso, 2012; Carmack et al., 2015). Sea ice velocity is increasing along
- with wind speeds (Kwok et al., 2013; Carmack et al., 2015). The Beaufort Gyre ice and ocean
- circulation intensified over 1995-2008, and then stabilized over 2008-2015 (McPhee et al., 2013;
- 103 Krishfield et al., 2014; Zhang et al., 2016; Armitage et al., 2017). Increased Ekman convergence
- during the spin up period led to freshwater accumulation within the upper 400 m (Proshutinsky
- et al., 2009; Krishfield et al., 2014), while the stabilization period has been associated with
- increased mixed layer salinity (Zhang et al., 2016). These recent dynamic changes, i.e. the
- stabilization of the Beaufort Gyre together with decreased sea ice extent in summer, have the
- 108 potential to influence the Canada Basin mixed layer.
- This paper focuses on the winter mixed layer, which is historically under-observed due to limited
- ship access in winter months. We are interested in the interannual and large-scale changes to the
- mixed layer, not the variations in mixing layers that are indicative of mixing over a number of
- days (see Section 3). Ice-Tethered Profiler observations since 2006 reveal that the decades long
- shoaling trend of the winter mixed layer in the Canada Basin has reversed.
- 114 2 Data
- 115 *2.1 Ice-Tethered Profilers*

- We utilize temperature and salinity profiles in the Canada Basin of the Arctic Ocean from Ice-
- 117 Tethered Profilers (Toole et al., 2011; downloaded in March 2019 from www.whoi.edu/itp). The
- region south of 80.5°N and west of 165°W in the Canada Basin is considered, limiting the
- analysis to the Beaufort Gyre region (see Regan et al., 2019). To focus on the winter mixed
- layer, January through May data for each ITP and year are treated as separate records. These
- months are selected to avoid months when the mixed layer may be seasonally deepening or
- shoaling. Only records longer than 30 days are used. A total of 36 winter records are available
- over 2006-2017 that meet these criteria (Figure 1), with further details of these records provided
- 124 in Table 1.
- Eight records do not yet have fully processed temperature and salinity data available; we use the
- level II data product for these records (Krishfield et al., 2008). Downward profiles are excluded
- from analysis of level II data, as these have known biases due to the profiler wake that are not
- corrected in this level of processing. The vertical resolution of the level II products is 2 dbar
- compared with 1 dbar for all other ITP data. A total of 12,148 profiles are included in the
- analysis, of which 1,065 are level II data. A direct comparison of level II upward profiles and the
- final (level III) data processing shows that differences in mixed layer depth or salinity are minor
- 132 (e.g., less than 1 m on average for mixed layer depth; not shown).
- The ITP systems record at least two (one upward, one downward) profiles of temperature and
- salinity each day. Some systems were programmed to sample more frequently in time, up to 8
- profiles per day, and so there are between 30 profiles (a single month of level II data) and 1200
- profiles (5 months of highly sampled data) within each of the 36 January May records (Table
- **137** 1).
- To evaluate potential changes to mechanical mixing within the mixed layer (as opposed to
- thermodynamically driven mixing), the ice velocity during each record is considered. Ice
- velocity is estimated from hourly GPS positions of the ITP surface unit. Ice velocity is then
- interpolated to the corresponding times of each profile, and the speed is then estimated.
- 142 *2.2 Ice concentration*
- 143 SSM/I ice concentration (Cavalieri et al., 1996) is utilized as it spans the entire record and is
- sufficient to show the interannual changes in January-May ice cover. Ice concentration was
- interpolated to the times and locations of the ITP profiles used in this analysis.

146 3 Methods

- 147 There is not a universal definition of mixed layer depth in the Arctic Ocean, and density
- thresholds of 0.01 to 0.25 kg m-3 appear in the literature (Toole et al., 2010; Timmermans et al.,
- 2012; Peralta-Ferriz and Woodgate, 2015). Here, three different potential density thresholds from
- the shallowest observation are considered: 0.03 kg m-3, 0.10 kg m-3, and 0.25 kg m-3. The mixed
- layer depth refers to the 0.25 kg m-3 density threshold, and is the focus of this study as it is
- indicative of the large-scale structure of the Beaufort Gyre. With this definition, mixed layer
- depth represents the depth to which water has mixed over the winter season and accurately tracks
- the region of elevated stratification and shear (Figure 2a-b). An alternate definition of mixed
- layer depth using a 0.10 kg m-3 density threshold was also considered, and all results are found to

- be robust to the choice of density threshold (see Section 5). In addition to these definitions of a
- mixed layer, we consider a mixing layer base defined using a density threshold of 0.03 kg m-3 for
- illustrative purposes. Mixing layer depth is representative of weak stratification within the mixed
- layer often associated with submesoscale fronts (Timmermans et al., 2012). We do not consider
- statistics of the mixing layer here. Note that due to the occasional presence of shallow mixing
- layers (e.g., Figure 2a-b), we consider statistics of the potential density at the base of the mixed
- layer (e.g., a mean value of 1021.6 kg m-3 for ITP-5; Figure 2a), which is greater than the
- average potential density within the mixed layer (e.g., a mean value of 1021.4 kg m-3 for ITP-5;
- 164 Figure 2a).
- 165 The shallowest observation was typically at ~7 m depth, although it was sporadically deeper for
- some profiles (e.g., Figure 2). Missing observations in the upper few meters were not crucial for
- determining the mixed layer depth in winter (whereas, in summer, they can be). Only six profiles
- were excluded from analysis due to insufficient data in the upper tens of meters.
- To evaluate interannual changes taking place in waters just beneath the mixed layer, the depth of
- the 1023.5 kg m-3 potential density surface is considered. It is the shallowest potential density
- surface present throughout all records, and often resides less than 10 m beneath the mixed layer
- base (e.g., Figure 2). Changes to the mean depth of the 1023.5 kg m-3 potential density surface
- are indicative of Ekman pumping in the uppermost portions of the halocline (see Section 4.1).
- To evaluate how a changing mixed layer may impact the ice cover, the heat content, and the
- amount of ice that heat can melt, are considered. Heat content relative to the freezing
- temperature is estimated for each profile as $Q = \rho_0 c_n \int (T T_f) dz$, where $\rho_0 = 1023$ kg m-3 is a
- reference value, $C_p = 3986 \text{ J kg}^{-1} \,^{\circ}\text{C}^{-1}$ the specific heat capacity, and T_f the freezing temperature
- of seawater. The reference salinity used in estimating the freezing temperature is the average
- salinity of the region considered, which is the 0.5 kg m-3 potential density range immediately
- beneath the mixed layer base (discussed further in Section 4). The amount of ice that can be
- melted is estimated as $\Delta z_{ice} = Q/\rho_{ice}/q_{lh}$ where ρ_{ice} =910 kg m-3 is the density of the ice, and
- 182 $q_{1h}=3\times10^5$ J kg-1 is the latent heat of fusion for sea ice.
- Liquid freshwater content is also estimated for each profile. Following Proshutinsky et al.
- 184 (2009), liquid freshwater content is estimated as $\int (S_{ref} S(z))/S_{ref} dz$ where a reference
- salinity of 34.8 g kg-1 is used (see also Aagaard and Carmack, 1989). The integral is calculated
- from 2 m depth to the depth at which salinity equals the reference salinity, with the shallowest
- salinity value extrapolated to 2 m depth (so that no portion of the upper water column is
- excluded). The reference salinity is at approximately 350-400 m depth, and so this is a relative
- measure of the freshwater in the upper ocean that can be used to investigate freshwater
- variability. The liquid freshwater content is also considered as the integral from 2 m to the 29.2 g
- 191 kg-1 salinity surface that resides a few meters beneath the base of the mixed layer (and
- corresponds to the 1023.5 kg m-3 potential density surface on average) to give an estimate of
- 193 freshwater content of this uppermost region.

4 Results

194

195

4.1 Mixed layer conditions

- 196 Representative ITP records from the central Beaufort Gyre (74-75°N, 140-153°W) illustrate the
- changes to winter mixed layer properties that occurred during 2006-2017 (Figure 2). Observed
- winter mixed layers sampled by ITP-80 in 2015 were 9 m deeper on average (40.2 m versus 31.0
- m) than those sampled by ITP-5 in 2007. Potential density surfaces in the halocline also
- deepened. The 1023.5 kg m-3 isopycnal, which was 7-8 m below the mixed layer base in both
- records, deepened by 11 m (39 m versus 50 m on average), suggesting downward Ekman
- pumping of the upper halocline between the ITP-5 observations in 2007 and the ITP-80
- observations in 2015. Mean potential density profiles show that the mixed layer became denser
- as well as deeper (Figure 2d), suggesting that some vertical mixing or increase in salinity
- occurred (due to a change in the freshwater budget, e.g., decreased melting or river runoff).
- The ITP dataset of 36 records for the January May period shows the interannual variability in
- 207 mixed layer depth (Figure 3a). Despite variability within (e.g., Figure 2a-b) and between records,
- the data reveal a clear interannual change with the shallowest winter mixed layers observed in
- 209 2008-2009, and the deepest winter mixed layers in 2014-2017. For detailed analysis, the data
- were partitioned into the time periods of 2006-2012 and 2013-2017. The two groups show a
- significant difference in the mixed layer depth distributions (Figure 3c). Mean mixed layer
- depths were 9.1 m deeper over 2013-2017 (mean \pm standard error of 39.3 \pm 0.1 m) versus 2006-
- 213 2012 (mean \pm standard error of 30.2 \pm 0.1 m).
- 214 Potential density surfaces in the upper halocline also deepened over 2006-2017. The 1023.5 kg
- 215 m-3 isopycnal had a mean depth of 38.8 m in 2006-2012, and 43.7 m in 2013-2017 (Figure 3a),
- an increase of 4.9 m (compared with an increase of 9.1 m for the mixed layer base). The
- 217 interannual variability of the depth of the 1023.5 kg m-3 isopycnal did not perfectly follow that of
- 218 the mixed layer, with the two variables exhibiting obvious co-variability only during 2013-2017.
- Deeper in the water column, the 1025.0 kg m-3 isopycnal had a mean depth of 62.7 m in 2006-
- 201 2012 and 64.2 m in 2006-2012, an increase of 1.5 m. For both the 1023.5 and 1025.0 kg m-3
- potential density surfaces, PDFs during the two time periods were significantly different at the
- 222 99% confidence interval (not shown).
- The mean density at the base of the mixed layer, ρ_{MLB} , was 0.51 kg m-3 denser over 2013-2017
- 224 (mean \pm standard error of 1022.34 \pm 0.01 kg m-3 versus 1022.85 \pm 0.01 kg m-3 over 2006-2012),
- consistent with vertical entrainment across the mixed layer base and/or a net reduction in
- freshwater input to the mixed layer (Figure 3b,d). Probability density functions (PDFs) of density
- at the mixed layer base were significantly different at the 99% confidence level (Figure 3d).
- 228 To address whether these density and salinity changes could have resulted from one-dimensional
- vertical mixing, artificial salinity and density profiles are constructed by vertically mixing the
- 230 2006-2012 mean salinity and density profiles by an additional 4 m (e.g., salinity profiles in
- Figure 4b). Four meters is chosen as it is the difference between the 9.1 m mixed layer deepening
- and 4.9 m of isopycnal deepening. The mean density profile vertically mixed in this way
- corresponded to a mixed layer potential density that increased by 0.08 kg m-3, less than one
- quarter of the observed increase in potential density between the two time periods. Note that
- vertically mixing by 9 m corresponds to a mixed layer potential density that increased by 0.25 kg
- 236 m-3, only half of the observed increase. Thus, a change in net freshwater input to the mixed layer
- is required to explain the observed increase in density at the base of the mixed layer.

Average profiles similarly show that the waters beneath the mixed layer also changed over the

study period (Figure 4). The subsurface temperature maximum of Pacific Summer Water that

resides at ~40-100 m depth increased by up to 0.6°C during 2013-2017 (Figure 4a, see also

241 Timmermans et al. 2018). The mixed layer became ~1 g kg-1 saltier, with nearly identical mean

salinity profiles below 60 m depth. The denser and deeper mixed layers over 2013-2017 resulted

in a stratification maximum at the mixed layer base that was weaker compared to the earlier

period. The upper ocean stratification in the Canada Basin (Figure 4c) was influenced by vertical

245 mixing and/or a reduction in freshwater input to the mixed layer that increased the density of the

246 mixed layer and the density at which the (weaker) stratification maximum occurred.

The heat content and average stratification of the region immediately beneath the mixed layer

base combine to determine the extent to which one-dimensional vertical mixing can melt sea ice.

Here we consider only what can be reasonably entrained, which is the 0.5 kg m-3 density span

below the mixed layer base that corresponds to the actual increase in mixed layer density over

251 2006-2017. This region represents the water mixed into the mixed layer for 2006-2012 profiles,

and the water that could be mixed into the mixed layer for 2013-2017 profiles assuming a similar

increase in mixed layer salinity were to occur in future years. The heat content relative to the

254 freezing temperature, Q (Section 3), and stratification in this region is estimated from individual

profiles. In the later time period, heat content had increased (Figure 5a) and average stratification

256 had decreased with fewer instances of both very weak and very strong stratification (Figure 5b),

consistent with changes to the mean profiles (Figure 4). The average heat content in the 0.5 kg

258 m-3 beneath the mixed layer base was 2.8 MJ m-2 over 2006-2012 versus 5.1 MJ m-2 over 2013-

259 2017, and is enough heat to melt 0.01 m (2006-2012) and 0.02 m (2013-2017) of ice. Compared

to the 0.6 m of net ice thinning that has occurred each decade (Carmack et al., 2015), vertically

261 mixing this heat into the mixed layer accounts for less than 3% of the total melt during 2006-

262 2012 (0.01 m) or during 2013-2017 (0.02 m assuming a continued increase in mixed layer

density). The average stratification beneath the mixed layer base decreased by 16% between the

264 time periods, making it energetically easier to vertically mix heat from the Pacific Summer

265 Water layer.

252

266

280

4.2 Ice conditions

To address whether the interannual deepening of the mixed layer depth resulted from interannual

268 changes to the ice cover (e.g., the presence of leads) that can influence vertical mixing, ice

269 concentration and ice speed are considered specifically for this spatial and temporal subset of the

270 region. Values were interpolated to the profile times and locations in Figure 1. The interannual

271 changes to ice concentration and speed are similar to those observed from instruments with more

272 complete coverage of the Canada Basin (Section 1). Ice concentrations during January – May

were above 90% in both time periods with a slightly higher probability of full ice cover (100%)

ice concentration) over 2013-2017 (Figure 6a). Ice speed increased during 2013-2017, with a

smaller proportion of ice speeds less than 0.05 m s-1 and median speeds of 0.07 m s-1 during

276 2013-2017 compared with 0.06 m s-1 during 2006-2012 (Figure 6b). Changes between the time

277 periods were significant at the 99% confidence level for ice speed and winter ice concentration.

278 At deployment, the initial ice thickness of the sea ice floe on which an ITP was deployed was

also recorded (a thickness of 0 m was specified for systems deployed in open water). Ice

thickness was measured in a variety of ways but the uncertainty is small compared to the bias

- 281 from preferentially deploying ITPs on the most robust ice available, and in summer (33 of the
- records were deployed in the August October period). The initial ice thickness estimates
- decreased from a mean \pm standard error of 3.2 \pm 0.1 m over 2006-2012 to 1.6 \pm 0.2 m over 2013-
- 284 2017 (not shown).

5 Discussion

- 286 *5.1 Robustness of results*
- 287 While the geographic coverage of the ITP records is not uniform, there is little evidence that
- 288 geographic variability influenced these results. Over the two time periods, observations are
- spread throughout the Beaufort Gyre, with similar changes observed in both individual records
- and the collective mean (Figures 2-4). Gridded maps of mixed layer depth and salinity show that
- these changes were large in scale, spanning the entire basin (Figure 7).
- These results are also robust to alterations in the methods used to analyze the ITP dataset,
- specifically the definition of the mixed layer base and the definition of winter. Considering a
- 294 mixed layer base defined using a 0.10 kg m-3 density threshold, as was used in Peralta-Ferriz and
- 295 Woodgate (2015), mixed layer depths in both time periods were slightly shallower on average
- 296 (Figure 8a), with only minor differences in the density at the mixed layer base (Figure 8b). The
- 297 mixed layer deepened by 10.7 m between the two time periods, a slightly larger change than
- when using a density threshold of 0.25 kg m-3 (9.1 m of deepening). Considering a stricter
- definition of winter to be only the months of January, February, and March, the probably density
- 300 functions of mixed layer depth remained largely unchanged with no significant changes to the
- mean mixed layer depth (Figure 8c). The increase in density at the mixed layer base between the
- two time periods was 0.46 kg m-3 for the January March subset of data, similar to the 0.51 kg
- 303 m-3 increase for the full January May dataset (Figure 8d).
- Alternate error estimates of mean mixed layer depth can be considered. We have given the
- standard error of the mean mixed layer depth in each time period assuming each profile is an
- independent measurement, which leads to a standard error of ± 0.01 m. Assuming that
- measurements are independent on a weekly basis results in N=353 and 307 degrees of freedom
- for 2006-2012 and 2013-2017, respectively, and a standard error of ± 0.3 m for both time periods.
- As the measurements have a 1-2 m vertical resolution, ± 1 m in 2006-2012 and ± 2 m in 2013-
- 2017 is an alternate error estimate. Even with this larger error estimate, the 9 m deepening of the
- 311 mixed layer remains significant.
- *5.2 Causes of a deeper, saltier, and denser winter mixed layer*
- 313 It is clear that some mechanisms are not solely responsible for the increase in mixed layer
- 314 salinity. All processes associated with one-dimensional vertical mixing cannot explain the
- observed changes to the mixed layer, including: an increase in winter ice growth and brine
- rejection, increased mechanical mixing, or reduced stratification at the stratification maximum
- that could increase entrainment.
- In further support of this conclusion, the indirect indicators of vertical mixing analyzed here,
- specifically ice speed and ice concentration that are indicative of leads at this time of year,
- 320 suggest that any changes to vertical mixing were not substantial. The observed increase in ice

321 speeds was weak, and moreover, ice speeds increased during the decadal spin-up of the Beaufort

Gyre while the mixed layer shoaled (Kwok et al., 2013; Peralta-Ferriz and Woodgate, 2015). As

323 there was a slight decrease between the two time-periods in the fraction of open water during

January – May, direct atmospheric forcing through leads (during these months) does not explain

325 the recent increase in mixed layer depth either. It is possible that the 2012 summer ice extent

326 minima introduced additional wind-forced mixing to the upper ocean, which then made it easier

327 to deepen the mixed layer base during the subsequent winter. This argument is weakened as a

similar ice extent minimum was observed in 2007 without a corresponding increase in mixed

layer depth in the following years. While a cumulative effect of decreased ice extent influencing

the mixed layer remains a possibility, ice extent can certainly have an indirect influence via

modulation of processes such as Ekman pumping and Ekman convergence of surface waters.

Overall, it is not possible, from our ITP data, to conclude whether the strength of vertical mixing

at the mixed layer base changed over 2006-2017.

336

358

Beyond the conclusion that vertical mixing is not the sole cause of increased mixed layer

salinity, the exact mechanism can only be speculated on from these observations. It is possible

that the stabilization of the Beaufort Gyre documented in recent studies led to increased mixed

layer salinities via a reduced Ekman convergence of freshwater (Zhang et al., 2016; Meneghello

et al., 2018; Zhong et al., 2018; Dewey et al., 2018), which made it easier for the "background"

level of mechanical mixing to deepen the mixed layer base. Alternatively, the increased mixed

layer salinity could have resulted from a net export of freshwater out of the Beaufort Gyre,

implying that the Arctic Ocean could increase freshwater export to the North Atlantic should

these conditions continue. Additional processes such as changing freshwater runoff and/or ice

growth in winter may be contributing along with changes in Beaufort Gyre circulation (driven by

changes in atmospheric circulation). This claim is supported by the increase in depth of the

345 uppermost density surfaces (by 1.5 to 5 m) over the two time periods (implying Ekman

convergence and downward Ekman pumping) alongside reduced mixed layer salinity (implying

347 Ekman convergence of saltier waters). Regardless of the exact mechanism behind the increase in

mixed layer salinity, the increased salinity is the most likely cause for the deeper mixed layers.

The simultaneous increase in mixed layer depth along with the downward displacement of

density surfaces over 2006-2017 differed from previous years. In the decades prior to 2008

during the spin-up of the Beaufort Gyre, the mixed layer shoaled (Peralta-Ferriz and Woodgate,

352 2015) while isopycnal depths increased (Timmermans et al., 2014; Zhang et al., 2016), compared

with mixed layer deepening and isopycnal deepening over 2013-2017. The deepening of

isopycnal surfaces even very near the base of the mixed layer is not a direct cause of the deeper

mixed layer during 2013-2017. Indirectly, if the stratification maxima had shoaled somewhat

during 2006-2017, changes in mixed layer depth would likely have been less dramatic, and so

isopycnal deepening aids mixed layer deepening.

5.3 Timing and interannual variability

359 There is some uncertainty in the exact timing of the increase in mixed layer depth. The

shallowest mixed layers in the analysis period occurred in 2008-2009, and the trend towards

361 greater winter mixed layer depths may have begun during these years (Figure 3a). This would be

consistent with the stabilization of the Beaufort Gyre circulation that began in 2008-2009

363 (Krishfield et al., 2014; Timmermans et al., 2014; Zhang et al., 2016; Dewey et al., 2018;

- Meneghello et al., 2018). We have chosen to present the change in mixed layer depth as between
- time periods of 2006-2012 versus 2013-2017 as this corresponds to the observed change in
- mixed layer density (Figure 3b), it approximately divides the ITP record in half, and corresponds
- to well separated statistics of mixed layer depth (Figure 3c).
- 368 The increase in mixed layer depth occurred over a period of less than five years, and suggests
- that the sparse winter observations available during the past 30 years may have undersampled
- 370 significant interannual variability. As a result, estimated trends of persistent decadal shoaling
- may be biased. Both existing and future numerical modeling studies should be used to
- investigate changes in mixed layer depth on interannual to decadal timescales. However, realistic
- 373 numerical modeling may be hindered due to the lack of spatially and temporally varying fields
- 374 (of river runoff for example) with which to force models in past decades.
- 375 *5.4 Cautions and implications*
- 376 A full picture of how the mixed layer has changed is only obtained by considering several
- measures of salinity, density, and freshwater. As noted previously, density at the base of the
- mixed layer differs from the average density of the mixed layer; the former is a better measure of
- entrainment potential, and the latter is indicative of changes to average density (or salinity)
- 380 conditions. There is also an important distinction between mixed layer salinity, which increased,
- and freshwater content, which decreased, between the two time periods. Liquid freshwater
- 382 content relative to S=34.8 g kg-1 (Section 3, ~400 m depth) was 20.6 m over 2006-2012 and 21.3
- m over 2013-2017, an increase of 0.7 m. Even when considering the region above the 29.2 g kg-1
- salinity surface (or approximately the 1023.5 kg m-3 isopycnal that consists of the mixed layer
- and a few meters of water beneath it), freshwater content increased (slightly) from 7.4 m over
- 386 2006-2012 to 7.5 m over 2013-2017. These uppermost tens of meters consist of waters that are
- saltier in comparison to previous years but fresher compared to waters below, so it is the
- deepening of the (relatively fresh) mixed layer that results in increased freshwater content.
- While we have focused on salinity and density, one consequence of a deepening mixed layer is
- 390 the potential erosion of any wintertime near-surface temperature maximum layer. There was no
- evidence of a winter-time near-surface temperature maximum (Maykut and McPhee et al., 1995;
- Jackson et al., 2010; Steele et al., 2011) within the mixed layer in the averaged winter-time
- temperature profiles for either time period (Figure 4a). Note that mixed layer temperature was
- 394 0.03°C cooler on average over 2013-2017 (Figure 4a), due to the increase in mixed layer salinity
- that reduced the freezing temperature of sea water. This is again in contrast to past observations
- of warming and freshening of the winter mixed layer (Jackson et al., 2011).
- Regardless of the exact cause of changes in mixed layer depth, there are implications for the
- 398 present and future Arctic system. It is inconclusive, from this analysis alone, whether or to what
- extent freshwater is being exported from the Beaufort Gyre, as an increase in mixed layer salinity
- 400 can also result from decreased ice melt, increased ice growth, or decreased river runoff. The
- reduced stratification and increased heat content over 2013-2017 suggests a future western Arctic
- where one-dimensional vertical mixing increasingly brings heat into the mixed layer. Even
- 403 though past observations (Maykut and McPhee, 1995; Shaw et al., 2009; Toole et al., 2010) and
- 404 the present study conclude that it is difficult to vertically mix Pacific Summer Water heat into the
- mixed layer to melt ice, this conclusion should continue to be re-evaluated in the future,

- 406 especially if mixed layer salinity increases further. Taking a three-dimensional view (as in
- Timmermans et al., 2014), the increased mixed layer density likely affects the proportion of
- 408 Pacific Summer Water that subducts more or less adiabatically beneath the mixed layer versus
- being incorporated within the mixed layer to impact the ice cover or warm the atmosphere. Had
- 410 the mixed layer continued to freshen and shoal, the Pacific Summer Water layer would likely
- 411 have contained even more heat than it does at present. The future evolution of the mixed layer
- and stratification at the base of the mixed layer will continue to influence, and be influenced by,
- 413 the evolution of the ice cover and upper ocean water masses.

6 Summary and Conclusions

- The changes observed over 2006-2017 are in contrast to those over 1980-2008. The observed
- 416 mixed layer reported here was 9 m deeper and ~1 g kg-1 saltier over 2013-2017 compared with
- 417 2006-2012. The increase in mixed layer salinity, and so in density, consequently weakened the
- stratification at the base of the mixed layer as well. This is a distinct change from the 0.64 m yr-1
- shoaling trend and 0.19 psu yr-1 freshening trend reported by Peralta-Ferriz and Woodgate
- 420 (2015).

414

- The changes to mixed layer depth were associated with increased mixed layer salinity that cannot
- be explained by one-dimensional vertical mixing. We therefore infer that changes to freshwater
- 423 storage and accumulation and/or release occurred between 2006 and 2017. These observations
- are insufficient to determine the cause of this salinity increase. However, it may have resulted
- from a decrease in the convergence of fresh surface waters ultimately driven by changes to
- 426 atmospheric circulation (e.g., Proshutinsky et al., 2009), or a convergence of saltier waters
- resulting from changes to river runoff or ice growth/melt. Continued downward Ekman pumping
- 428 of the upper density surfaces did not oppose the increase in mixed layer depth, and potentially
- 429 made it easier for existing mechanical mixing to deepen the mixed layer base as the freshwater
- eroded. Our understanding of the Arctic system would be improved by monitoring several
- aspects of the ocean in addition to freshwater storage, including ocean turbulence and vertical
- 432 mixing.

433

Acknowledgments

- We gratefully acknowledge J. Toole for helpful conversations. S. Cole was supported by the
- National Science Foundation under grant number PLR-1602926, and J. Stadler by the Woods
- 436 Hole Oceanographic Institution Summer Student Fellowship program. Profile data is available
- via the Ice-Tethered Profiler program website: http://whoi.edu/itp. SSM/I ice concentration data
- was downloaded from the National Snow and Ice Data Center.

439 References

462 463

464

465

467

468 469

- 440 Aagaard, E., and E. C. Carmack (1989), The role of sea ice and other fresh water in the Arctic 441 circulation, J. Geophys. Res., 94, 14485-14489.
- 442 Armitage, T. W. K., S. Bacon, A. L. Ridout, A. A. Petty, S. Wolbach, and M. Tsamados (2017), 443 Arctic Ocean surface geostrophic circulation 2003-2014, Cryosphere, 11, 1767-1780.
- 444 Carmack, E., I Polyakov, L. Padman, I. Fer, E. Hunke, J. Hutchings, J. Jackson, D. Kelley, R. 445 Kwok, C. Layton, H. Melling, D. Perovich, O. Persson, B. Ruddick, M.-L. Timmermans, 446 J. Toole, T. Ross, S. Vavrus, and P. Winsor (2015), Toward quantifying the increasing 447 role of oceanic heat in sea ice loss in the new Arctic, Bull. Amer. Meteor. Soc., 96, 2079-448
- 449 Cavalieri, D. J., C. L. Parkinson, P. Gloersen, and H. Zwally (1996, updated 2017), Sea ice concentrations from Nimbus-7 SSMR and DMSP SSM/I-SSMIS passive microwave data, 450 version 1, Boulder, Colorado USA: NASA National Snow and Ice Data Center 451 452 Distributed Active Archive Center, doi: 10.5067/8GQ8LZQVL0VL.
- 453 Comiso, J. C. (2012), Large decadal decline in the Arctic multiyear ice cover, J. Climate, 25, 454 1176-1193.
- 455 D'Asaro, E. A., and J. H. Morison (1992), Internal waves and mixing in the Arctic Ocean, Deep-456 Sea Res., 39, S459-S484.
- 457 Dewey, S., J. Morison, R. Kwok, S. Dickinson, D. Morison, and R. Andersen (2018), Arctic ice-458 ocean coupling and gyre equilibration observed with remote sensing, Geophys. Res. Lett., 459 45, 1499-1508.
- Guthrie, J. D., J. H. Morison, and I. Fer (2013), Revisiting internal waves and mixing in the 460 Arctic Ocean, J. Geophys. Res., 118, 3966-3977. 461
 - Jackson, J. M., E. C. Carmack, F. A. McLaughlin, S. E. Allen, and R. G. Ingram (2010), Identification, characterization, and change of the near-surface temperature maximum in the Canada Basin, 1993-2008, J. Geophys. Res., 115, C05021.
- Jackson, J. M., S. E. Allen, F. A. McLaughlin, R. A. Woodgate, and E. C. Carmack (2011), Changes to the near-surface waters in the Canada Basin, Arctic Ocean from 1993-2009: 466 A basin in transition, J. Geophys. Res., 116, C10008.
 - Krishfield, R., J. Toole, and M.-L. Timmermans (2008), ITP data processing procedures. Woods Hole Oceaongraphic Institute Tech Rep., 24 pp, available at http://www.whoi.edu/fileserver.do?id=35803&pt=2&p=41486.
- 471 Krishfield, R. A., A. Proshutinsky, K. Tateyama, W. J. Williams, E. C. Carmack, F. A. McLaughlin, and M.-L. Timmermans (2014), Deterioration of perennial sea ice in the 472 Beaufort Gyre from 2003 to 2012 and its impact on the oceanic freshwater cycle, J. 473 474 Geophys. Res., 119, 1271-1305.
- Kwok, R., G. F. Cunningham, M. Wensnahan, I. Rigor, H. J. Zwally, and D. Yi (2009), Thinning 475 476 and volume loss of the Arctic Ocean sea ice cover: 2003-2008, J. Geophys. Res., 114, 477 C07005.
- 478 Kwok, R., G. Spreen, and S. Pang (2013), Arctic sea ice circulation and drift speed: Decadal 479 trends and ocean currents, J. Geophys. Res., 118, 2408-2425.
- 480 Maykut, G. A., and M. G. McPhee (1995), Solar heating of the Arctic mixed layer, J. Geophys. 481 Res., 100, 24691-24703.
- 482 McPhee, M. G. (2012), Advances in understanding ice-ocean stress during and since AIDJEX, 483 Cold Reg. Sci. Tech., 76-77, 24-36.

- McPhee, M. G. (2013), Intensification of geostrophic currents in the Canada Basin, Arctic Ocean, J. Climate, 26, 3130-3138.
- Meneghello, G., J. Marshall, M.-L. Timmermans, and J. Scott (2018), Observations of seasonal
 upwelling and downwelling in the Beaufort Sea mediated by sea ice, J. Phys. Oceanogr.,
 488 48, 795-805.
- Peralta-Ferriz, C., and R. A. Woodgate (2015), Seasonal and interannual variability of pan-Arctic surface mixed layer properties form 1979 to 2012 from hydrographic data, and the dominance of stratification for multiyear mixed layer depth shoaling, Prog. Oceaongr., 134, 19-53.
- 493 Proshutinsky, A., R. Krishfield, M.-L. Timmermans, J. Toole, E. Carmack, F. McLaughlin, W. J.
 494 Williams, S. Zimmerman, M. Itoh, and K. Shimada (2009), Beaufort Gyre freshwater
 495 reservoir: State and variability from observations, J. Geophys. Res., 114, C00A10.
- Regan, H. C., C. Lique, and T. W. K. Armitage (2019), The Beaufort Gyre extent, shape, and location between 2003 and 2014 from satellite observations, J. Geophys. Res., 124, 844-862.
- Shaw, W. J., T. P. Stanton, M. G. McPhee, J. H. Morison, and D. G. Martinson (2009), Role of the upper ocean in the energy budget of Arctic sea ice during SHEBA, J. Geophys. Res., 114, C06012.
- Steele, M. W. Ermold, and J. Zhang (2011), Modeling the formation and fate of the near-surface temperature maximum in the Canadian Basin of the Arctic Ocean, J. Geophys. Res., 116, C11015.
 - Timmermans, M.-L., S. Cole, and J. Toole (2012), Horizontal density structure and restratification of the Arctic Ocean surface layer, J. Phys. Oceanogr., 42, 659-668.

- Timmermans, M.-L., A. Proshutinsky, E. Golubeva, J. M. Jackson, R. Krishfield, M. McCall, G.
 Platov, J. Toole, W. Williams, T. Kikuchi, and S. Nishino (2014), Mechanisms of Pacific
 Summer Water variability in the Arctic's Central Canada Basin, J. Geophys. Res., 119,
 7523-7548.
- Timmermans, M.-L., J. Toole, and R. Krishfield (2018), Warming of the interior Arctic Ocean linked to sea ice losses at the basin margins, Sci. Adv., 4, eaat6773.
- Toole, J. M., M.-L. Timmermans, D. K. Perovich, R. A. Krishfield, A. Proshutinsky, and J. A.
 Richter-Menge (2010), Influences of the ocean surface mixed layer and thermohaline
 stratification on Arctic Sea ice in the central Canada Basin, J. Geophys. Res., 115,
 C10018.
- Toole, J. M., R. A. Krishfield, M.-L. Timmermans, and A. Proshutinsky (2011), The Ice-Tethered Profiler: Argo of the Arctic, Oceanogr., 24, 126-135.
- Zhang, J., M. Steele, K. Runciman, S. Dewey, J. Morison, C. Lee, L. Rainville, S. Cole, R.
 Krishfield, M.-L. Timmermans, and J. Toole (2016), The Beaufort Gyre intensification and stabilization: A model-observation synthesis, J. Geophys. Res., 121, 7933-7952.
- Zhong, W., M. Steele, J. Zhang, and S. T. Cole (2018), Circulation of Pacific Winter Water in
 the western Arctic Ocean, J. Geophys. Res., 124, 863-881.

Table 1. Details of the Jan-May ITP records used in this analysis.

Record	ITP	Year	Dates	Processing	Number of
Number _a	number	1 cai	Dates	Trocessing	Profiles _b
1	ITP-1	2006	1/1 - 5/31	Final	602
2	ITP-3	2006	1/1 - 5/31	Final	597
3	ITP-5	2007	1/1 - 5/31	Final	393
4	ITP-6	2007	1/1 - 5/31	Final	297
5	ITP-4	2007	1/1 - 5/31	Final	300
6	ITP-8	2008	1/1 - 5/31	Final	301
7	ITP-13	2008	1/1 - 5/31	Final	314
8	ITP-18	2008	1/1 - 5/31	Final	274
9	ITP-8	2009	1/1 - 5/31	Final	148
10	ITP-11	2009	1/1 - 5/31	Final	314
11	ITP-33	2010	1/1 - 5/31	Final	275
12	ITP-34	2010	$\frac{1/1-3/31}{1/1-3/30}$	Final	175
13	ITP-32	2010	1/1 - 2/9	Final	76
14	ITP-35	2010	1/1 - 3/31	Final	514
15	ITP-43	2011	1/1 - 2/11	Final	41
16	ITP-41	2011	1/1 - 5/31	Final	296
17	ITP-42	2011	1/1 - 4/15	Final	200
18	ITP-53	2012	1/1 - 5/31	Final	278
19	ITP-41	2012	1/1 - 5/31	Final	301
20	ITP-62	2013	1/1 - 5/31	Final	275
21	ITP-65	2013	1/1 - 5/31	Final	426
22	ITP-64	2013	1/1 - 5/31	Final	418
23	ITP-70	2014	1/1 - 5/31	Final	1203
24	ITP-69	2014	1/1 - 2/15	Final	46
25	ITP-77	2014	3/10 - 5/31	Final	657
26	ITP-78	2014	3/11 - 5/31	Final	649
27	ITP-79	2014	3/21 - 5/31	Final	569
28	ITP-80	2015	1/1 - 5/24	Final	1144
29	ITP-85	2015	1/1 - 5/31	Level II	151
30	ITP-81	2015	1/1 - 5/31	Level II	151
31	ITP-86	2015	1/1 - 5/31	Level II	149
32	ITP-87	2015	1/1 - 5/31	Level II	148
33	ITP-82	2015	1/1 - 5/31	Level II	151
34	ITP-82	2016	1/1 - 3/10	Level II	47
35	ITP-89	2016	1/1 - 5/31	Level II	121
36	ITP-97	2017	1/1 - 5/31	Level II	147

^aRecords are arranged in the order in which they are plotted in Figure 3a-b. ^bNumber of profiles with a mixed layer depth estimate.

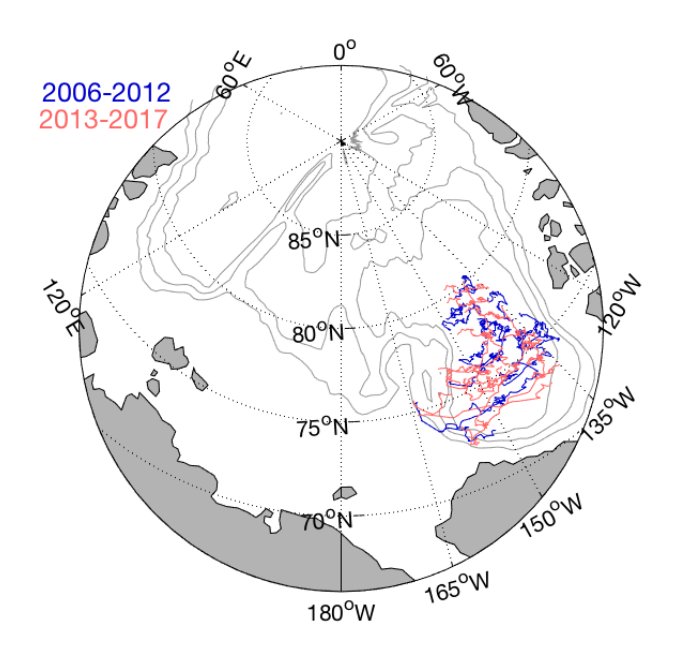


Figure 1. Map of each Jan –May ITP record during 2006-2012 (blue) and 2013-2017 (red).

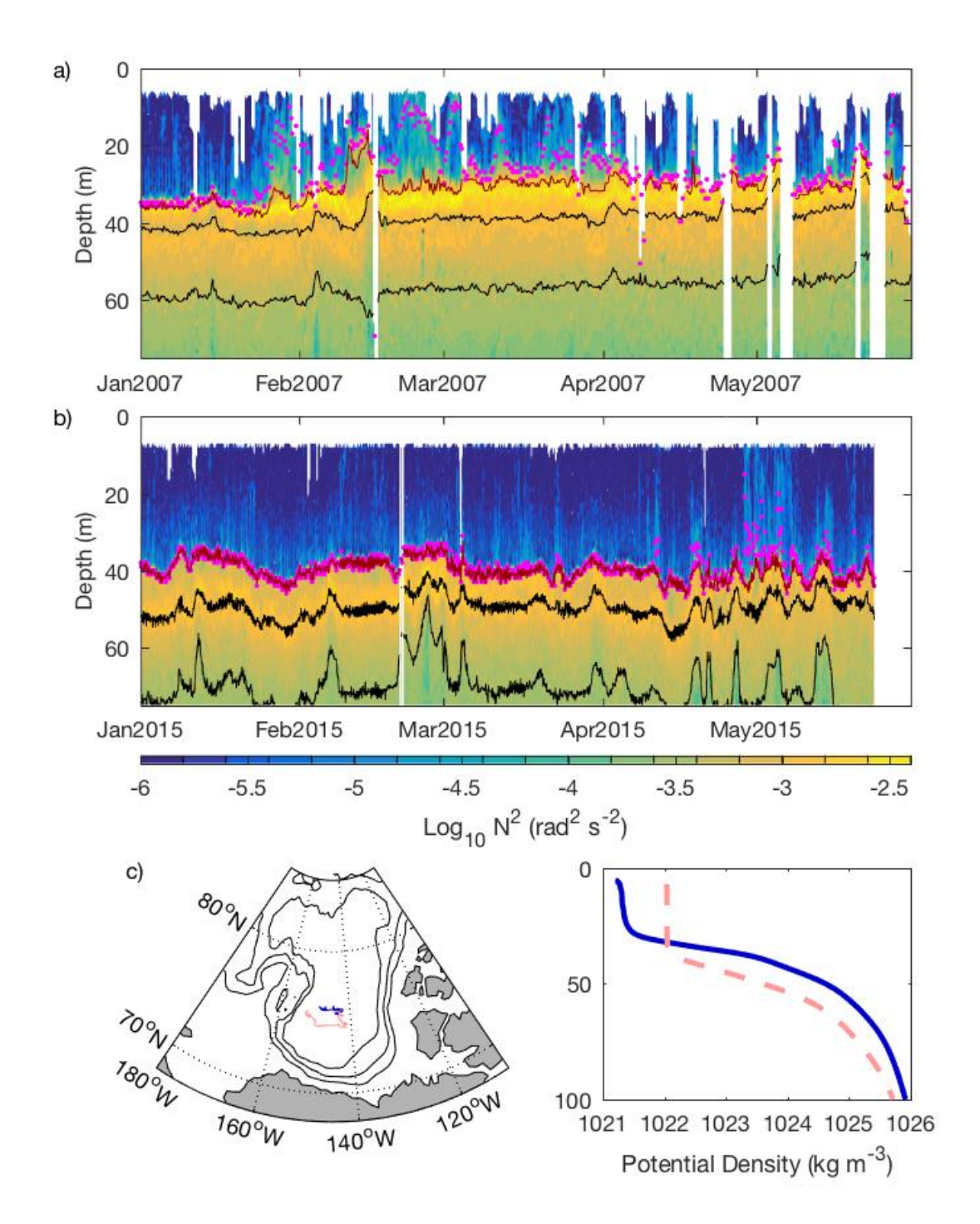


Figure 2. Example time series of buoyancy frequency for a) ITP-5 in 2007 and b) ITP-80 in 2015. The mixed layer base (dark red line) and mixing layer base (magenta dots) are estimated using 0.25 kg m-3 and 0.03 kg m-3 potential density thresholds, respectively, and sometimes coincide. The 1023.5 kg m-3 and 1025.0 kg m-3 potential density surfaces (black) are also shown. Note that ITP-5 profiled twice per day while ITP-80 profiled eight times per day causing the black and dark red lines to appear thicker for ITP-80 as internal wave variability is resolved in more detail. c) Map of profile locations and d) average potential density for ITP-5 (blue) and ITP-80 (red).

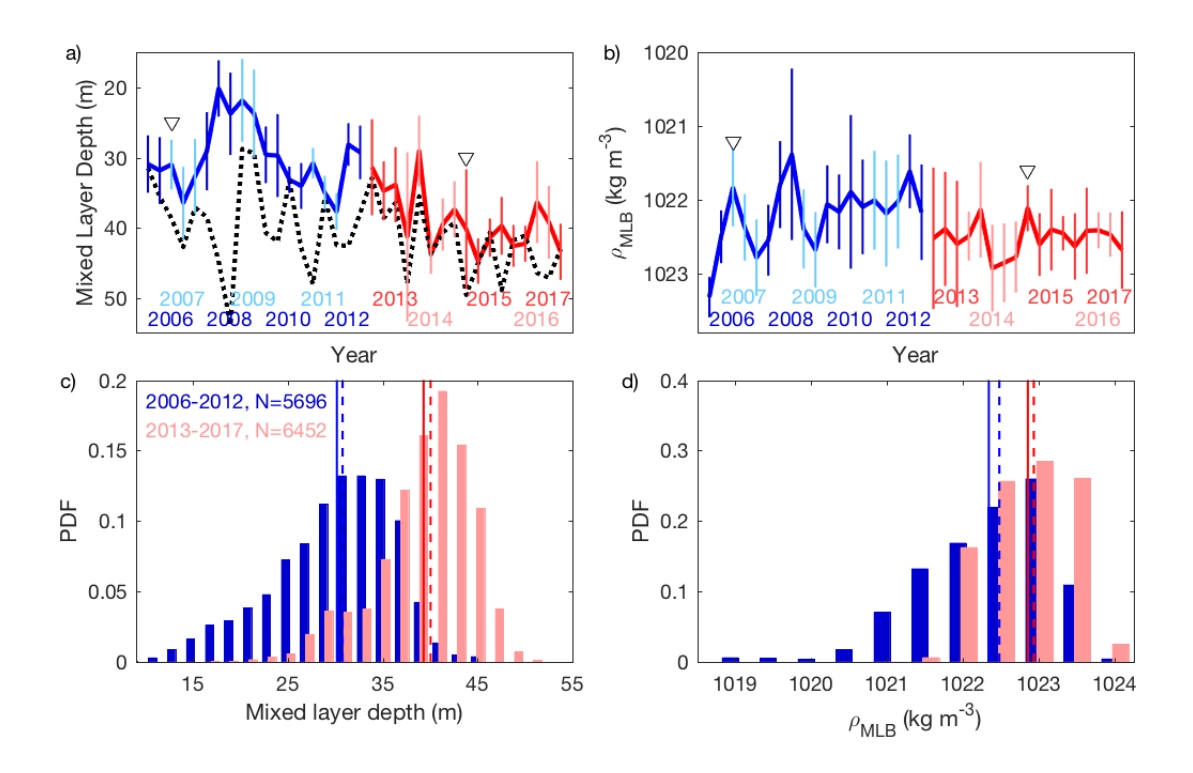


Figure 3. Mean (thick line) and standard deviation (thin vertical bars) for each January-May record of a) mixed layer depth and b) density at the mixed layer base, ρ_{MLB} . Blue denotes 2006-2012 and red 2013-2017 with each year in light or dark shading and records plotted in the order listed in Table 1. Triangles indicate ITP-5 and ITP-80 records shown in Figure 2. The mean depth of the 1023.5 kg m-3 density surface (dotted black) is shown in (a). Probability density functions (PDFs) over 2006-2012 and 2013-2017 of c) mixed layer depth with the total number of profiles indicated, and d) density at the mixed layer base. Mean (solid) and median (dashed) values are indicated for each time period.

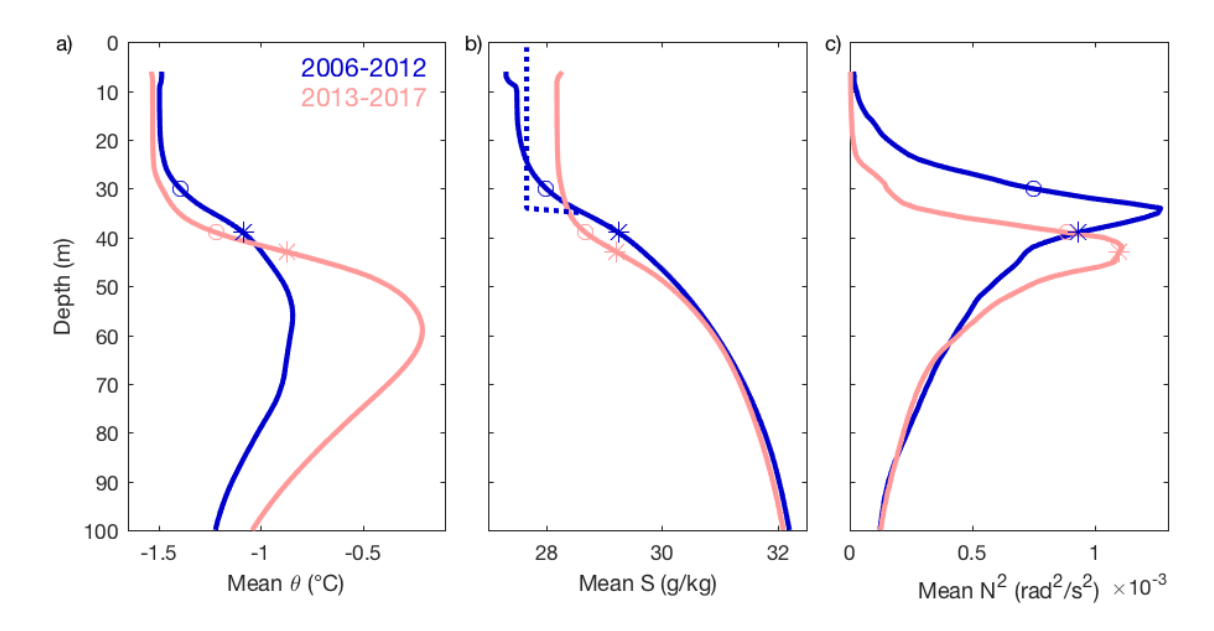


Figure 4. Average a) potential temperature, b) salinity, and c) stratification profiles over 2006-2012 (blue) and 2013-2017 (red). The mean properties at the mean mixed layer depth (circles) and at 1023.5 kg m-3 (asterisks) are indicated for each period. Dotted blue line in (b) is the salinity profile of the 2006-2012 data after vertically mixing by an additional 4 m.

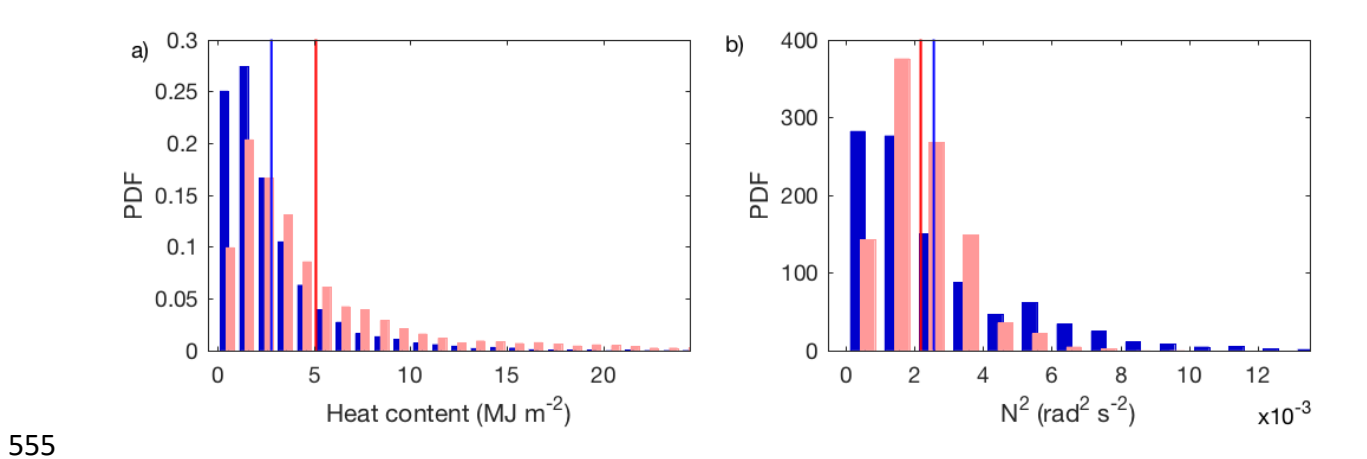


Figure 5. Probability density functions over 2006-2012 (blue) and 2013-2017 (red) of average a) heat content and b) stratification of the 0.5 kg m-3 density range immediately beneath the mixed layer base. Mean (solid) and median (dashed) values are indicated for each time period.

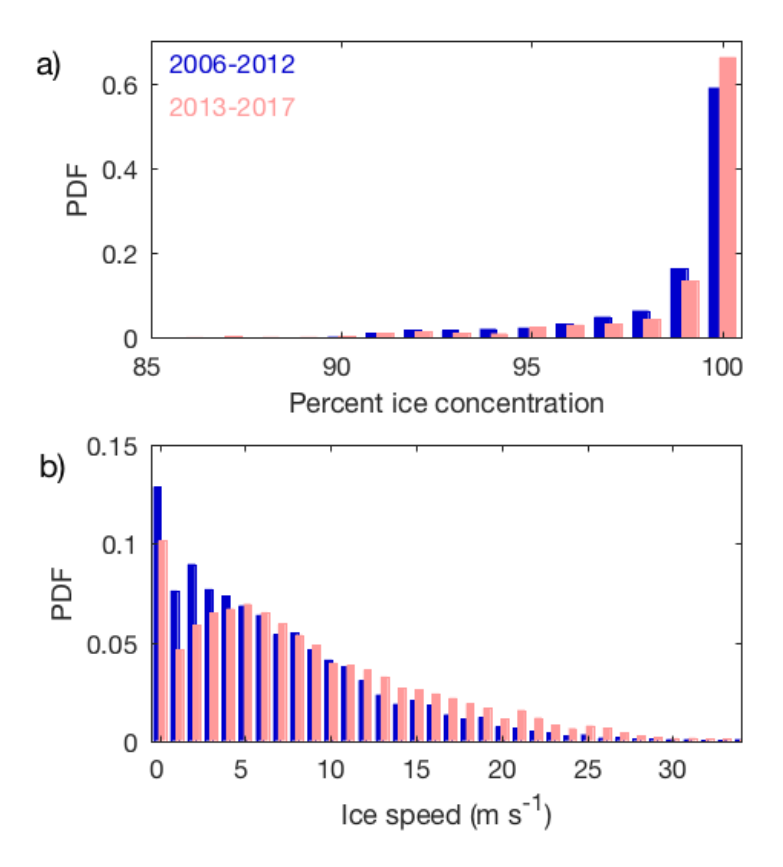


Figure 6. Ice conditions during 2006-2012 (blue) and 2013-2017 (red) showing probability density functions of a) ice concentration, and b) ice speed.

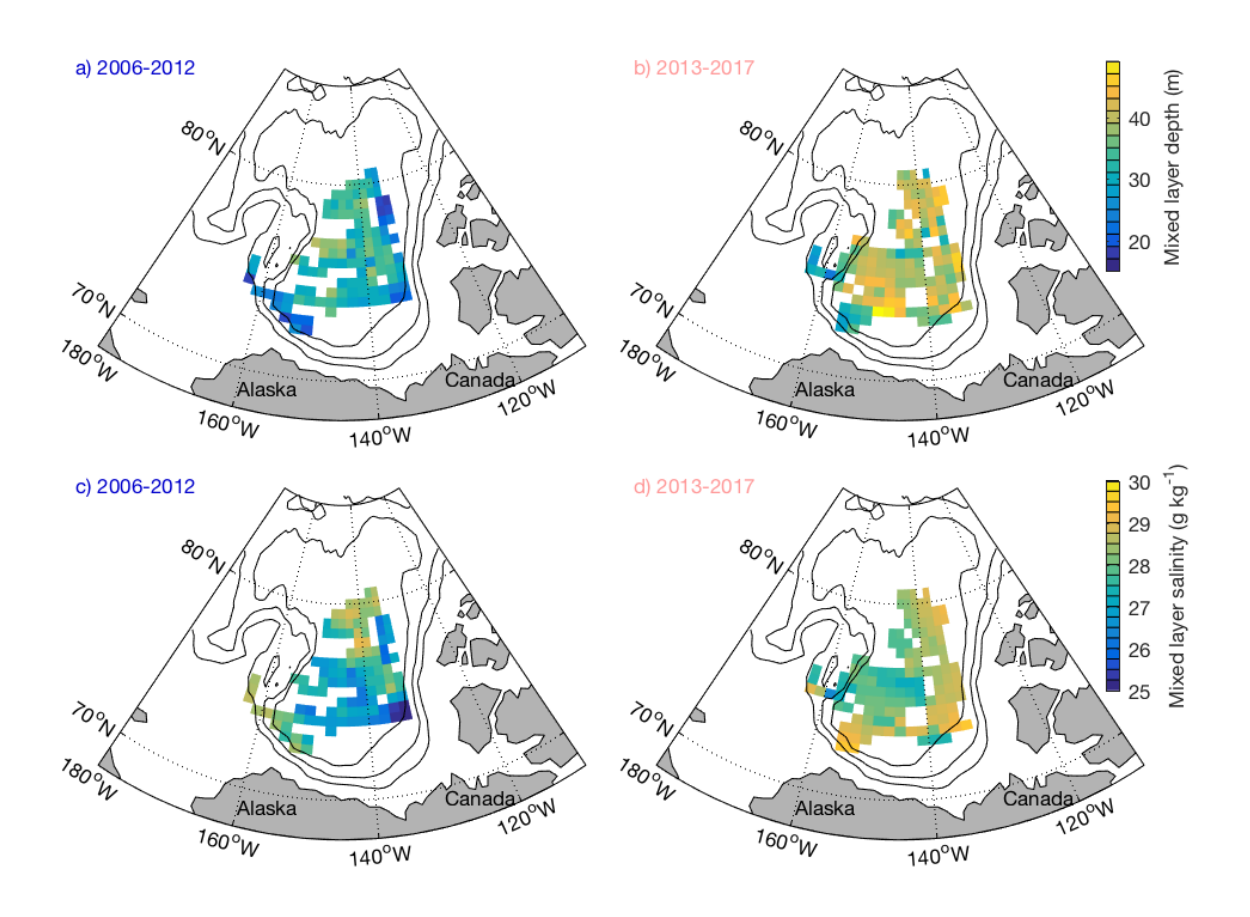


Figure 7. Gridded averages of a-b) mixed layer depth and c-d) salinity at 10 m depth over a,c) 2006-2012 and b,d) 2013-2017. Spatial gridding was done by averaging all data into bins of 2° in longitude and 0.5° in latitude (or approximately 56x58 km bins at these latitudes).

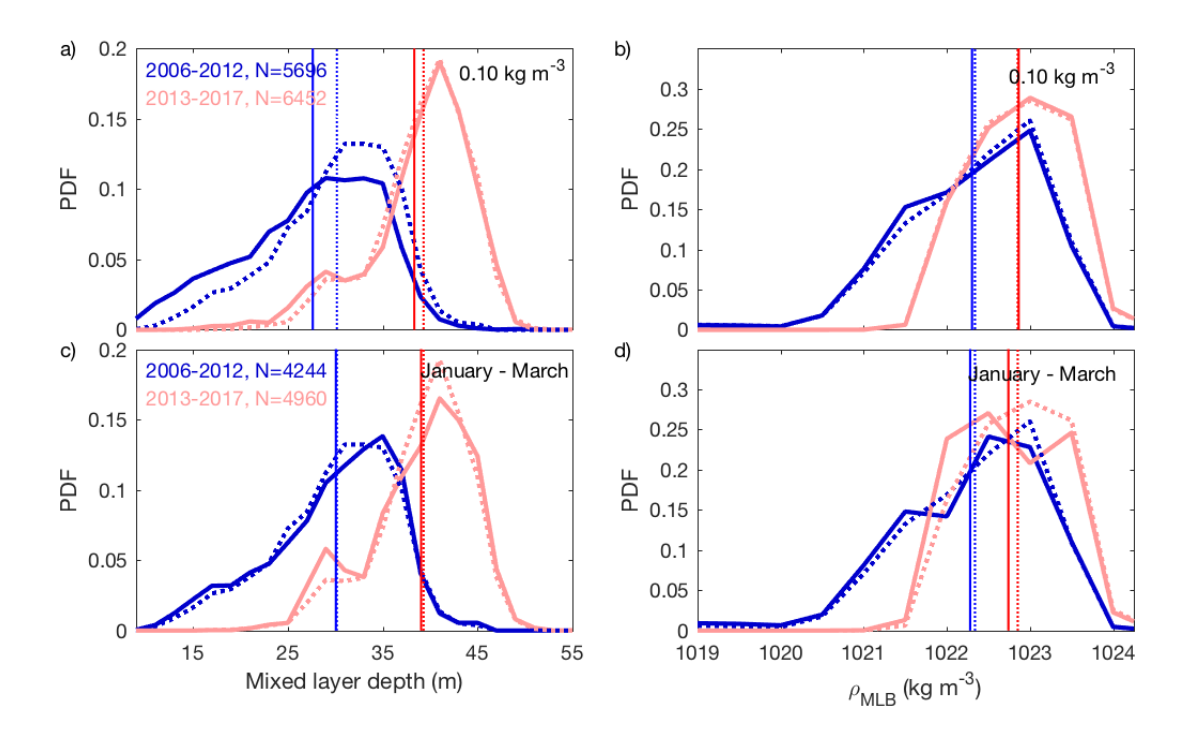


Figure 8. Probability density functions (PDFs) over 2006-2012 and 2013-2017 of a,c) mixed layer depth with the total number of profiles indicated, and b,d) density at the mixed layer base. In a-b), a mixed layer defined using the 0.25 kg m-3 density threshold (dotted; as in Figure 3c-d) is compared to a 0.10 kg m-3 density threshold (solid). In c-d), the full January — May dataset (dotted; as in Figure 3c-d) is compared with a subset of the data that includes only January — March profiles (solid). Mean values are indicated for each time period (solid and dotted).